Acta Biomed 2007; 78; Suppl 1: 99-112

Lecture

^{13}C NMR isotopomeric analysis and its application in the study of endocrine cell metabolism and function

Nicholas E. Simpson, Ioannis Constantinidis
Division of Endocrinology, Department of Medicine, The University of Florida, FL, USA

Abstract. Defining mechanisms and enzymatic paths critical to cellular function (e.g., secretion) of endocrine cells is a key research goal that can lead toward novel avenues of therapeutic intervention for a variety of disorders. ^{13}C NMR spectroscopy and isotopomer analysis of cell extracts are excellent tools to quantitatively assess metabolism through intermediate labeling and estimate carbon entry to the TCA cycle. Discussed are: cell lines and in vitro culturing; extraction of intracellular material; NMR spectroscopy of the extract; isotopomeric analysis and modeling to obtain relative metabolic fluxes to the TCA cycle. This paper describes issues related to the application of NMR spectroscopic techniques on cell line extracts. Included are results of two studies that illustrate considerations that must be taken when performing analogous studies on neuroendocrine tissue: one involving the effect of media composition on cell behavior and isotopomer labeling; the second looking at effects of applying different metabolic models to ^{13}C data and inferences that may be drawn. NMR isotopomeric analysis is a powerful technique that may be applied to better understand endocrine cell function. (www.actabiomedica.it)

Key words: Isotopomer analysis, metabolism, NMR spectroscopy, secretion, TCA cycle

Abbreviations

α-KG, alpha-ketoglutarate; ACS, acetyl-CoA acetyltransferase; ALT, alanine aminotransferase; AST, aspartate aminotransferase; LDH, lactate dehydrogenase; ME, malic enzyme; NMR, nuclear magnetic resonance; OAA, oxaloacetate; PBS, phosphate buffered saline; PC, pyruvate carboxylase; PDH, pyruvate dehydrogenase; PEP, phospho*enol*pyruvate carboxylase; PK, pyruvate kinase; TCA, tricarboxylic acid.

Introduction

There are many aspects of neuroendocrinology that need to be addressed. One of these is to better understand the relationship between cell function and bioenergetics (i.e., the link between the cell's energetic machinery and the ability to secrete hormones). This may be particularly important in pituitary adenomas, whose metabolic requirements and bioenergetic machinery could differ from those of normal tissue, and impact the function of the tissue. Presently, there are methods readily available to study many aspects of cellular metabolism on in vitro systems. For example, oxygen consumption rates, glucose and lactate production rates, hexokinase/glucokinase enzymatic characteristics, and Ca^{++} flux can all be studied and related to secretion under a variety of physiological conditions. However, the addition of ^{13}C NMR spectroscopic techniques (on cellular extracts) to this analytical arsenal provides a powerful means by which substantial metabolic information concerning cellular energetics can be obtained, particularly information regarding that occurring in the mitochondria. Properly analyzed NMR spectroscopic data may be related to information gleaned from other assays to give a more complete view of intracellular bioenergetics and its relationship to the function of the cell.

This NMR technique has been used in a variety of cell systems to tease out biochemical information (1-10). The bulk of these studies have been performed in model insulin-secreting cell lines (i.e., insulinomas) and attempt to determine critical links between cellular energetics and cellular function (e.g., insulin secretion). However, the study of other model cell systems has been enhanced by the application of isotopomer analysis; specifically, the metabolic consequences of an enzyme deficiency and its treatment in fibroblasts (11). In theory, there is no reason why one cannot pursue similar studies with endocrine tissues. For example, one could study the pathogenesis of disease, or identify novel molecular targets. Armed with a basic metabolic knowledge of critical steps of metabolism important to cellular function (e.g., secretion), new avenues of therapeutic intervention may be tested to up- or down-regulate these critical metabolic steps. To aid the reader in appreciating the NMR technique, following is a simplistic description of how the complex NMR signals arise.

NMR spectroscopy and isotopomer analysis

Although it's a vastly oversimplified statement, atoms with nuclei that possess a nuclear spin (angular momentum) can be manipulated within a magnetic field to create the NMR phenomenon, and obtain signal. The growing discipline of magnetic resonance (which includes both spectroscopy and imaging) takes advantage of this phenomenon to obtain vast amounts of diverse information; biochemical, structural (chemical), anatomical, etc., depending on the experiment performed. For a complete description of the NMR phenomenon, the following books are suggested to the reader (12, 13).

As stated earlier, NMR spectroscopy is a powerful tool by which one can obtain bioenergetic information. One method is through studying changes in the carbon labeling of compounds involved in metabolic pathways. Although the usual isotope of carbon (^{12}C) is not NMR-detectable (i.e., it has no nuclear spin), the non-radioactive isotope ^{13}C does have a nuclear spin, and is readily NMR-observable. Because this isotope of carbon has an extremely low natural abundance, feeding cells a metabolizable label that includes ^{13}C is essential for detection and analysis. If a ^{13}C label is given to cells (e.g., ^{13}C-labeled glucose), the carbon label will enter the cell, and be distributed among various compounds reflective of the processes of metabolism. A standard model of glucose metabolism (14, 15), including glycolysis and pyruvate entry to the TCA cycle, is shown in Figure 1. In this model, following our example of stimulation with ^{13}C-uniformly-labeled glucose, glucose is metabolized to pyruvate through glycolysis. Glycolysis turns molecules of uniformly-labeled glucose into molecules of uniformly-labeled pyruvate, which have a number of potential metabolic fates. Among these are: 1) conversion to lactate (via lactate dehydrogenase: LDH); 2) conversion to alanine (via alanine aminotransferase, ALT); 3) entrance to mitochondria and the TCA cycle either by conversion to acetyl-CoA via the pyruvate dehydrogenase complex (PDH), or anaplerotic carbon entry via PC to form oxaloacetate (OAA). This cytosolic pyruvate pool can also be replenished from TCA cycle intermediates malate or OAA by malic enzyme (ME) or phospho*enol*pyruvate carboxylase

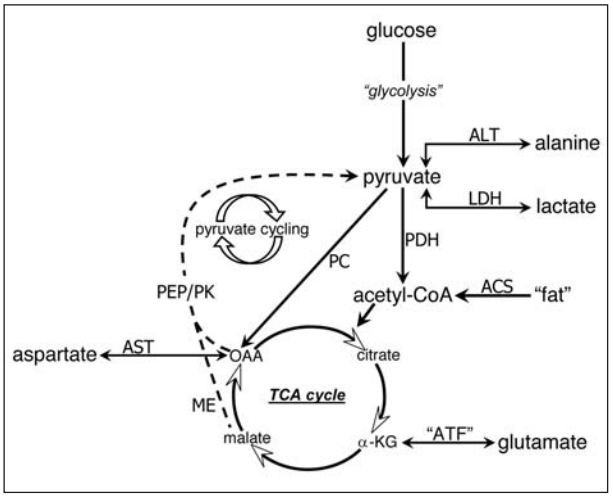

Figure 1. Standard model of glucose metabolism. In this model, glucose is metabolized to pyruvate through glycolysis, and then has a number of potential fates. Important enzymes include: ALT (alanine transaminase); LDH (lactate dehydrogenase); PDH (pyruvate dehydrogenase complex); PC (pyruvate carboxylase); ACS (acetyl-CoA acetyltransferase); AST (aspartate transaminase); "ATF" (aminotransferase); ME (malic enzyme); PEP/PK (phospho*enol*pyruvate carboxylase/pyruvate kinase)

(PEP)/pyruvate kinase (PK), respectively. Also of significance are α-ketoglutarate (α-KG) and aspartate. Conversion between aspartate and OAA is mediated by aspartate aminotransferase (AST). α-KG can be converted to the amino acid glutamate via glutamate dehydrogenase (which also can catalyze the reverse reaction). The exchange between these two species is also mediated by aminotransferases (ALT or AST).

An approach to determine the carbon flux through metabolic pathways by NMR spectroscopic means is by analyzing the carbons of glutamate, an amino acid and 5-carbon TCA cycle byproduct. When adjacent carbons are labeled, complex carbon multiplet resonance patterns emerge due to ^{13}C-^{13}C spin-spin interactions, or J-coupling. Analysis of these isotopomer patterns provides a quantitative assessment of metabolism and determines information regarding carbon entry to the TCA cycle (i.e., 'flux' through critical enzymatic steps) (16-18). Figure 2A outlines a simple example of how isotopomeric patterns arise. In this example, only the signals potentially arising from the 4th carbon of glutamate are considered. If the 4th carbon (C4) is labeled, but has no immediate neighboring carbons (C3 or C5) with a label, a single peak results (a singlet). In all cases, it is irrelevant what labeling occurs in non-neighboring carbons (C1 or C2, in this example). If the labeled C4 has a neighboring labeled C3, two peaks arise (a doublet). Likewise, if a labeled C4 has a neighboring C5 that is labeled, another doublet arises at a slightly different separation. This shift differs from the other doublet due to local chemical differences. Lastly, the labeled C4 carbon may have both neighbors labeled, giving rise to four peaks (a quartet). The distribution of each of these four possibilities (termed the fractional enrichment) dictates how the final resultant pattern will appear. For example, if each possibility is equal in number (e.g., 25% for each), the pattern for the glutamate C4 carbon will appear as depicted in Figure 2B. Likewise, the glutamate C4 pattern would appear as depicted in Figure 2C for the different stated fractional enrichment. Similar isotopomeric patterns arise from each glutamate carbon (C1, C2, C3, C4 and C5). These patterns are vital to determine the contributions of key enzymatic reactions in glucose metabolism. Because the paths by which labeled substrates enter (and re-enter) the TCA cycle impacts the scrambling of the carbon label, the steady-state isotopic labeling patterns of many TCA cycle intermediates and end-products reflect the contributions of the labeled and non-labeled substrates as well as the relative flux of the various entry ports into the TCA cycle (via PDH,

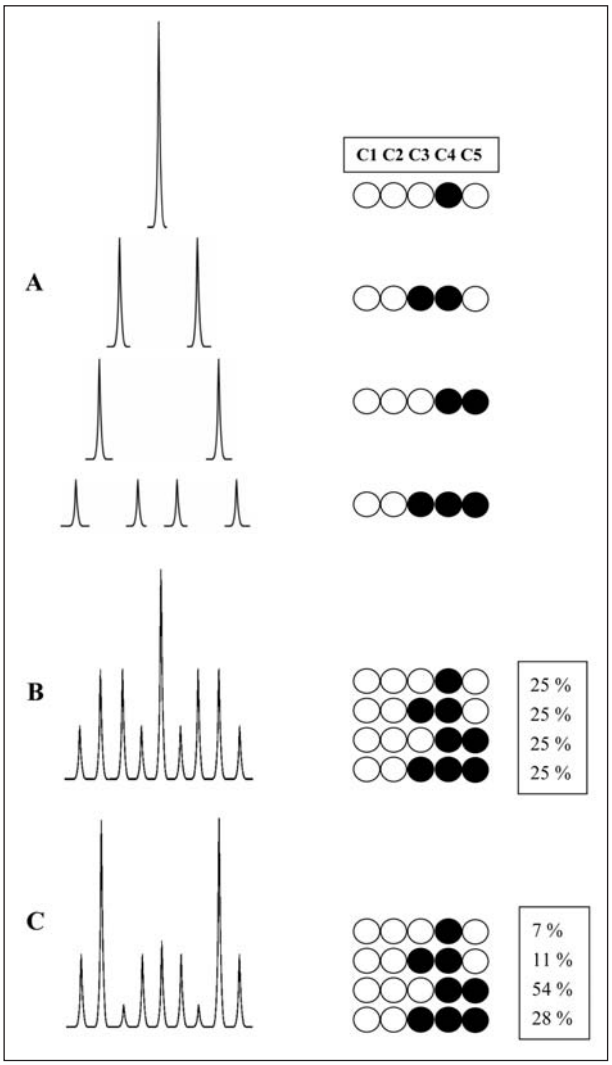

Figure 2. ^{13}C isotopic splitting. Panel A depicts an example of how neighboring labeled carbon atoms influence the isotopomeric splitting of a selected labeled 4th carbon of glutamate (C4). Dark circles represent labeled carbon, and open circles represent unlabeled carbon. Shown are the individual possible signals arising from a labeled 4th carbon as a consequence of labeling of the immediate neighbors. Panel B illustrates the resultant pattern of C4 glutamate if the labeled neighboring carbons have the fractional enrichment stated to the right of the figure. Panel C illustrates the resultant glutamate C4 pattern with a different fractional enrichment

PC or other anaplerotic pathways). In other words, by observing the isotopomeric patterns of glutamate, and analyzing (by hand or computer) the fractional enrichment, one can predict how the carbon must have entered the TCA cycle, and thus obtain estimates of TCA cycle metabolic flux.

Proper application of this NMR spectroscopic isotopomer analytical technique requires consideration of several factors. In this paper, we draw from our experience with insulin secreting cell lines and identify two potential pitfalls that must be considered when using the NMR isotopomeric approach. The first one (study 1) involves the effect of media on cell behavior and integration of the carbon label. The second (study 2) looks at the effects of applying different metabolic models to ^{13}C data and discusses inferences that may be drawn when using an appropriate model. However, this paper does not explicitly discuss any data related to pituitary research. Rather, this paper describes the promising applicability of the technique to analogous cell systems (such as neuroendocrine adenomas) for studying links between metabolism and secretion in a tissue of interest.

Materials and Methods

Cells

INS-1 (832/13) rat insulinoma cells were obtained from Christopher Newgard (Duke University, Durham, NC). Cells were cultured as monolayers in RPMI-1640 (Mediatech, Herndon, VA) and fed media every 2-3 days. The growth media contained ~11 mM glucose and was supplemented with 10% FBS (Hyclone, Logan, UT), antibiotics (100 U/ml penicillin and 100 μg/ml streptomycin), 2 mM Hepes, 2 mM L-glutamine, 1 mM sodium pyruvate and 50 γM β-mercaptoethanol (Sigma, St. Louis, MO). All cultures were grown at 37° C under humidified (5% CO_2/ 95% air) conditions.

^{13}C labeled incubation media

Three different incubation media were tested on the insulinoma cultures: PBS, containing no nutrients other than the added labeled glucose; incomplete media (RPMI-1640) containing labeled glucose and a supplement of glutamine and antibiotics described above, but no sera; and complete media containing the label and a full supplement of sera. The incubation media contained either 3 or 15 mM uniformly-labeled ^{13}C-glucose. These media created a variety of conditions to study metabolic links to secretion. The pH of all solutions was maintained at 7.2 to eliminate a potential pH effect on insulin release (19, 20). Cells were rinsed with glucose-free PBS, incubated in glucose–free PBS for 1.5 h, and rinsed again in glucose-free PBS prior to receiving the ^{13}C-labeled incubation media and being exposed for 4 hours.

Cell extraction

Four to six confluent T-175 flasks were used for each extraction. A representative flask of each trial helped determine the approximate number and viability of monolayer cultures through Trypan Blue exclusion and manual cell counting. After the incubation period, extracts were created as described by Tyagi et al. (21). Flasks were rinsed with ice-cold saline to remove residual extracellular media, extracted with ice-cold methanol and scraped off the flask. The methanol cell slurry was collected and equal volumes of chloroform and water were added. The aqueous portion was isolated, treated with Chelex-100 (Sigma, St. Louis, MO) to remove paramagnetics or compounds that would negatively impact the NMR signal, lyophilized, resuspended in 450 μl of D_2O (Cambridge Isotopes, Cambridge, MA), and placed in a 5 mm NMR tube.

Assays

Media samples were drawn from each flask at the start and conclusion of the incubation periods and assayed for glucose (all studies). Glucose concentrations were determined on a Vitros DT60II Bioanalyzer (Ortho-Clinical Diagnostics, Rochester, NY). Rates of glucose consumption (GCR) were calculated from the change in glucose levels during the incubation period. The rate of insulin release (ISR) was determined from media samples drawn at the start and at 20 mi-

nutes into the exposure. These were assayed with a commercially available double-antibody EIA kit (Linco Research, St. Charles, MO) measured on a Synergy HT plate reader (Bio-Tek, Winooski, VT).

NMR spectroscopy

NMR data were acquired using a 5 mm broadband receiving coil in an 11.75 Tesla vertical bore Bruker Avance-500 equipped with a ^{1}H decoupling channel (Bruker, Billerica, MA). A coaxial insert containing dioxane (^{13}C) and TMP (^{31}P) acted as a chemical shift and concentration reference. Acquisition parameters were: ^{13}C- sweep width, 30 kHz; repetition time, 6 s; number of transients, 10240. ^{31}P- sweep width, 8.09 kHz; repetition time, 6 s; number of transients, 1024. Waltz ^{1}H decoupling was applied throughout the acquisitions. Areas under the ^{31}P resonances of the α-ATP and α-ADP were determined by line-fit analysis with the program 'Nuts' (AcornNMR, Fremont, CA) and the ATP/ADP ratios calculated. ^{13}C NMR spectra were analyzed as described below.

^{13}C isotopomeric analysis

Area calculations of the isotopomer patterns of the C2, C3, C4 and C5 glutamate resonances in the ^{13}C NMR spectra were performed by line-fit analysis (Acorn NMR, Fremont, CA). Correction factors were applied to glutamate signal areas to correct for relaxation and nuclear Overhauser effects. Isotopomeric modeling analysis using the patterns and the C3/C4 ratio was performed with 'tcaCALC' (16-18), a program which uses algebraic equations to describe glutamate isotopomeric labeling patterns in terms of pathway fluxes of an applied metabolic model. Monte-Carlo simulations and non-linear least-squares analysis of the contributions of the various glutamate resonance multiplets determined the following metabolic information: the ratio of pyruvate going through PC vs. PDH ('YPC'); the fraction of labeled pyruvate carbons; the % of acetyl CoA derived from a pyruvate pool; the replenishment of pyruvate from TCA cycle intermediates ('PK'); and the amount of non-PC anaplerotic carbon entrance to the TCA cycle. The % anaplerosis is defined as the relative carbon entry from both anaplerotic pathways to the total carbon entering the TCA cycle. Pyruvate cycling is defined as the average of 'YPC' and 'PK' flux rates (2, 4). All rates are relative to the TCA cycle (i.e., entrance via citrate synthase), defined as 1.

Metabolic models

Metabolic models applied in 'tcaCALC' included a standard single-pyruvate pool model of glucose metabolism without (*'simple'*) and with a second *('modified'*) anaplerotic entrance, as shown in Figure 3A, and a dual-pyruvate pool model described by Lu et al. (2) represented in Figure 3B. The *'simple'* model is essentially the standard model of metabolism which was described earlier in the introduction (Fig. 1). Fully-labeled pyruvate is formed from the uniformly-labeled glucose and can enter the TCA cycle via PC or PDH. Unlabeled acetyl-CoA can be synthesized through other sources via acetyl-CoA acetyltransferase (ACS). Lastly, carbon units from the TCA cycle can replenish the pyruvate pool (represented by PK in the 'tcaCALC' program, but which includes pyruvate derived from malate or OAA via ME or PEP & PK).

The dual-pyruvate pool model as described by 'tcaCALC' (Fig. 3B) is more difficult to model and requires some redefining of terms. Here, glucose is metabolized to a primary pyruvate pool that enters the TCA cycle predominantly through acetyl-CoA (i.e., PDH), while another pyruvate pool predominantly cycles to the TCA cycle as defined earlier. To model this in 'tcaCALC', the substrate that creates uniformly-labeled acetyl-CoA is redefined as uniformly-labeled 'fat12'. However, rather than 'fat12' representing the two-carbon acyl groups that enter the metabolic cycle, we define the ACS activity here to represent the PDH activity on the primary pyruvate pool. A second pyruvate pool is derived from TCA cycle intermediates (defined as PK) that re-enter the TCA cycle via PC or PDH. Contribution to acetyl-CoA via PDH activity from this second pool indicates communication (mixing) between these two pyruvate pools. Pyruvate cycling is modeled only between the secondary pool and the TCA cycle.

The *'modified'* single-pyruvate pool model depicted in Fig. 3A includes the addition of non-PC ana-

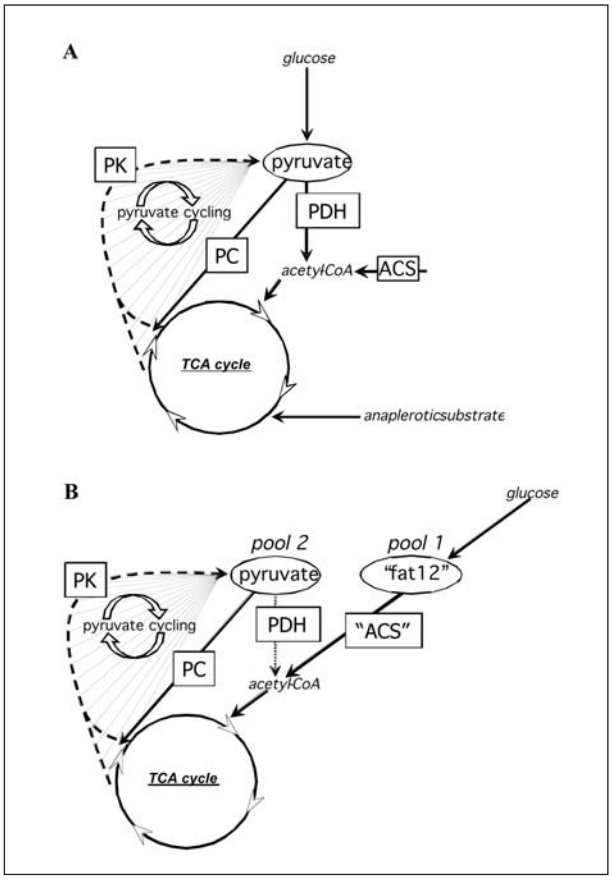

Figure 3. Schematics of the models of metabolism used by the program 'tcaCALC'. Panel A depicts both single pyruvate pool models. In the *'simple'* model, glucose metabolizes to a pyruvate pool, which enters the TCA cycle via PDH or PC. There may also be contribution to acetyl-CoA through ACS from unlabeled sources. The *'modified'* model includes the depicted additional anaplerotic substrate entrance to the TCA cycle. Panel B shows how parameters in 'tcaCALC' can be redefined to represent the dual-pyruvate pool model. Here, "fat12" and "ACS" are used to represent the uniformly-labeled pyruvate pool (pool 1) and PDH, respectively. Pyruvate is defined as a secondary pool (pool 2), which enters the TCA cycle through PC, and through which pyruvate cycling occurs. PDH here represents possible communication between the two pools, and is generally low, indicating little communication between the two defined pyruvate pools. In all models, pyruvate cycling is defined as the circulation of carbons between the TCA cycle and the pyruvate pool. This effectively adds partial labels to the pyruvate carbons in the pool. PK represents all re-entry to the pyruvate pool from TCA cycle sources and includes potential contributions from ME and PEP/PK enzyme systems

plerotic entrance to the TCA cycle from undefined labeled carbon sources. Anaplerosis from the pyruvate pool to the TCA cycle is through PC activity (to OAA) as well as potential conversion to malate via malic enzyme (ME). In all models used in the analysis, the sum of PDH + ACS is defined as 1. The term 'anaplerotic substrate' depicted on the figure represents any anaplerotic carbon entrance into the TCA cycle from sources other than pyruvate (e.g., aspartate, glutamate). Anaplerosis from the pyruvate pool to the TCA cycle includes PC activity (to OAA) as well as potential conversion to malate via ME. Therefore, the total anaplerosis includes that from aspartate, glutamate or pyruvate, and the % anaplerosis is defined as the relative carbon entry from both anaplerotic pathways to the total carbon units entering the TCA cycle. Pyruvate cycling is defined as the average of the anaplerotic entrance from the pyruvate pool and the PK flux rate, as per Lu et al (2). A paper detailing finer aspects of modeling with the program 'tcaCALC' is discussed elsewhere (18).

Statistical methods

For groups within a set of data (e.g., PBS, incomplete and complete media incubation groups), means and standard deviations were calculated, and a homoscedastic Student's t-test (two-tailed) for independent samples was performed. Relationships between data (e.g., GCR vs. ISR) were tested with the Pearson product-moment correlation.

The percentage errors of the glutamate C3/C4 ratio between the measured NMR data and modeled estimates were tabulated by the formula:

% C3/C4 error = 100 * [modeled (C3/C4) – measured (C3/C4)] / [measured (C3/C4)].

A heteroscedastic (two-sample, unequal variance) Student's t-test was performed on the model-derived residuals and % C3/C4 errors for each cell line to test whether different metabolic models provide similar values when applied to the same data. An F-test was performed on the standard deviations of the model-derived % C3/C4 errors and residuals to test whether different metabolic models provide similar precisions when applied to the same data. Relationships between data (e.g., ISR vs. PC activity, total anaplerosis, non-PC anaplerosis, etc.) were tested with the Pearson product-moment correlation.

Results and Discussion

Study 1

An important consideration when performing functional studies is to define the conditions under which cells should be studied to best reflect the in vivo situation. This is true for any cell system being studied. Following is an example of the impact that media selection has on cell function and metabolism in an insulin-secreting cell line, and how media composition influences the NMR spectra and isotopomer data.

It is known that fuel metabolism is required for insulin secretion (22), and a widely accepted mechanism for glucose stimulated insulin secretion termed the Fuel Hypothesis has been postulated (22-25), but the precise metabolic coupling factors to secretion are not yet fully understood. To this end, ^{13}C NMR spectroscopic studies on the metabolism of insulin-secreting cells have been performed. However, given the complexity of the resultant patterns and the need to obtain high spectral resolution, laboratories generally perform ^{13}C studies in buffered salts (2, 26-28) or media that does not contain sera (29-32). This occurs routinely despite published studies on insulin secreting cells that found that culture media and factors present in added serum affect the insulin secretion of the cells (33, 34). Consequently, most studies on the dynamic relationship between insulin release and cellular bioenergetics are not relevant to the in-vivo situation. Because it is reasonable to assume that as incubation media becomes more complex (with the addition of amino acids, fatty acids, vitamins and other co-factors), not only is the function of the cell altered, but metabolic pathways are altered to accommodate these nutrients. Consequently, the isotopomeric labeling patterns will be altered as well.

Figure 4 illustrates the effect that media complexity has on the integration of carbons derived from ^{13}C-glucose in INS-1 cells. Shown are representative ^{13}C spectra acquired from extracts of INS-1 cells exposed to PBS, incomplete media (no sera), or complete media (10% sera), each containing 15 mM labeled glucose. Incubation with labeled media yields resonances from a variety of metabolites. The most preva-

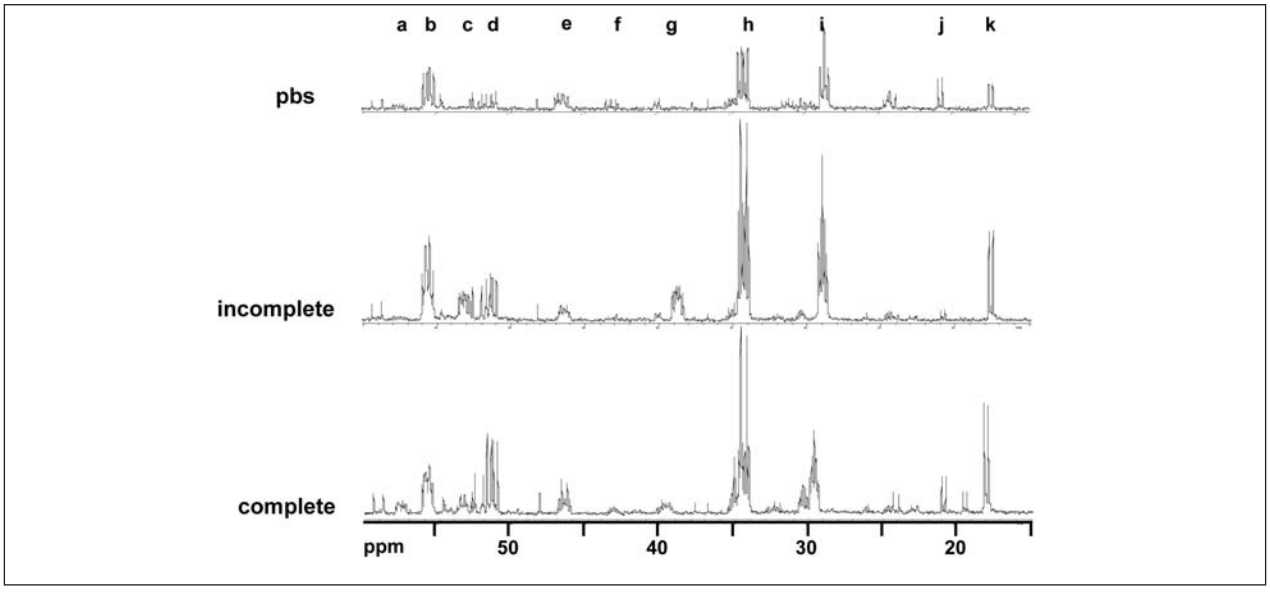

Figure 4. Representative proton-decoupled ^{13}C-NMR spectra obtained from extracts of INS-1 monolayer cultures exposed to PBS, incomplete media or complete media conditions containing 15 mM uniformly-labeled ^{13}C-glucose. Spectra are shown with equivalent S/N. On the x-axis at the bottom of the figure is the chemical shift region between 15 and 60 ppm. Species of interest are lettered, and include: (**a**) serine C2; (**b**) glutamate C2; (**c**) aspartate C2; (**d**) alanine C2; (**e**) citrate C2 & C4; (**f**) glycine C2; (**g**) aspartate C3; (**h**) glutamate C4; (**i**) glutamate C3; (**j**) lactate C3; and (**k**) alanine C3

lent metabolite produced by the INS-1 cells is glutamate (resonances b, h and i), implying that much of the glucose label is metabolized to pyruvate and enters the TCA cycle. This preference is reinforced by the profound lack of lactate produced (j), suggesting that lactate dehydrogenase activity is low, a characteristic that is far different from most other insulin-secreting cell lines. A substantial amount of alanine is visible (resonances d and k), indicating alanine transaminase activity, as is aspartate (resonances c and g), indicating aspartate transaminase activity. Additionally, the amino acid serine (resonance a), glycine (resonance f), as well as citrates (resonance e), are observed. Some other small resonances not yet assigned are also detected.

Visual inspection reveals striking differences in resonance signal intensities as a function of media complexity, with many detectable resonances increasing with media complexity. This is clearly the case for glutamate (b, h and i), serine (a), alanine (k), and some of the unassigned resonances. This indicates that label integration is enhanced by the presence of unlabeled compounds in the media such as amino acids or fatty acids and substances found in sera. Unusual changes are noted in the aspartate resonances (c and g), as they increase from PBS-exposure levels upon exposure to incomplete media, but again decrease upon exposure to complete media.

Figure 5 shows the isotopomer patterns of glutamate carbons (C2, C3 and C4) under three different media compositions, each containing 15 mM labeled glucose. This figure clearly indicates large differences in the isotopomeric patterns, and thus the fractional enrichment (this concept is outlined in Figure 2). In general, under PBS conditions, most carbons are labeled, leading to more quartets and triplets (where applicable), and less singlet. However, under complete media conditions, where the unlabeled amino acids and fatty acids present in the media are non-negligible components, less contiguous labeling occurs, resulting in a rise in singlets and doublets (where applicable). Differences in these patterns are attributable to differences in key enzymatic reactions of glucose metabolism, and these are examined in study 2.

When the glucose concentration is altered, but not the media complexity, the labeling of most amino acids and other metabolites increased or maintained

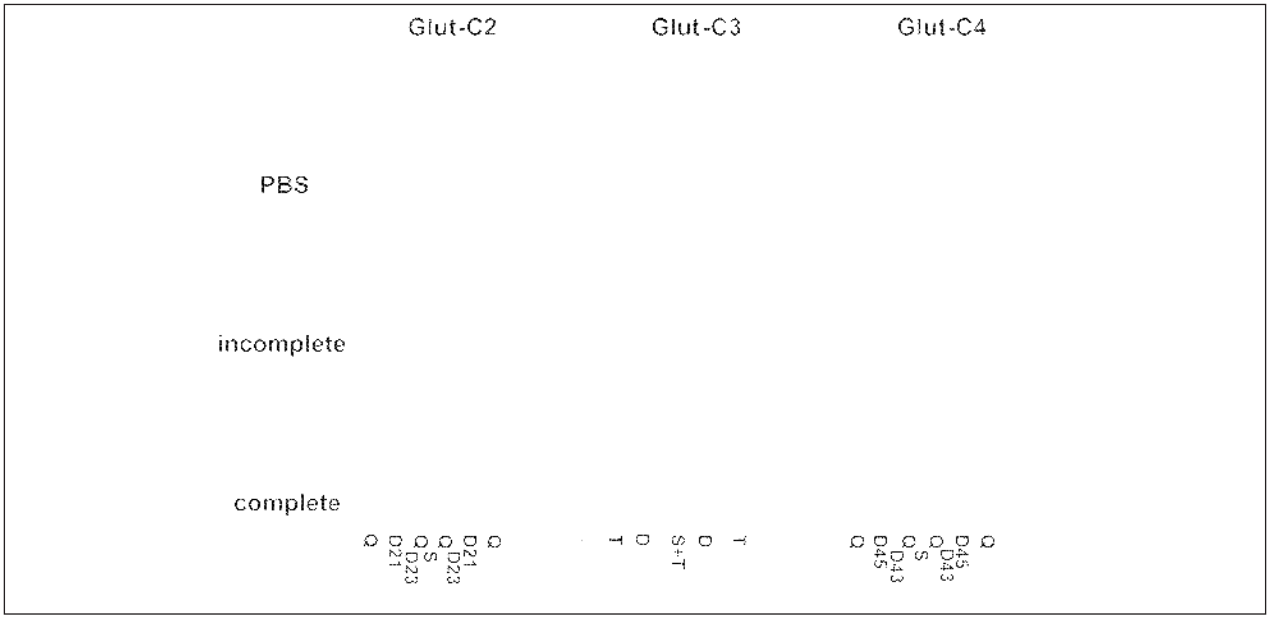

Figure 5. Proton-decoupled ^{13}C-NMR spectra of glutamate obtained from extracts of INS-1 monolayer cultures exposed to PBS, incomplete media or complete media conditions containing 15 mM uniformly-labeled ^{13}C-glucose. Under the lowermost representative glutamate carbon 2, 3, and 4 isotopomer patterns are symbols delineating from where the peaks arise. **S** represents the singlet; **D** the doublet; **Q** the quartet, and **T** the triplet (actually a quartet with the two middle components coincidental with the singlet)

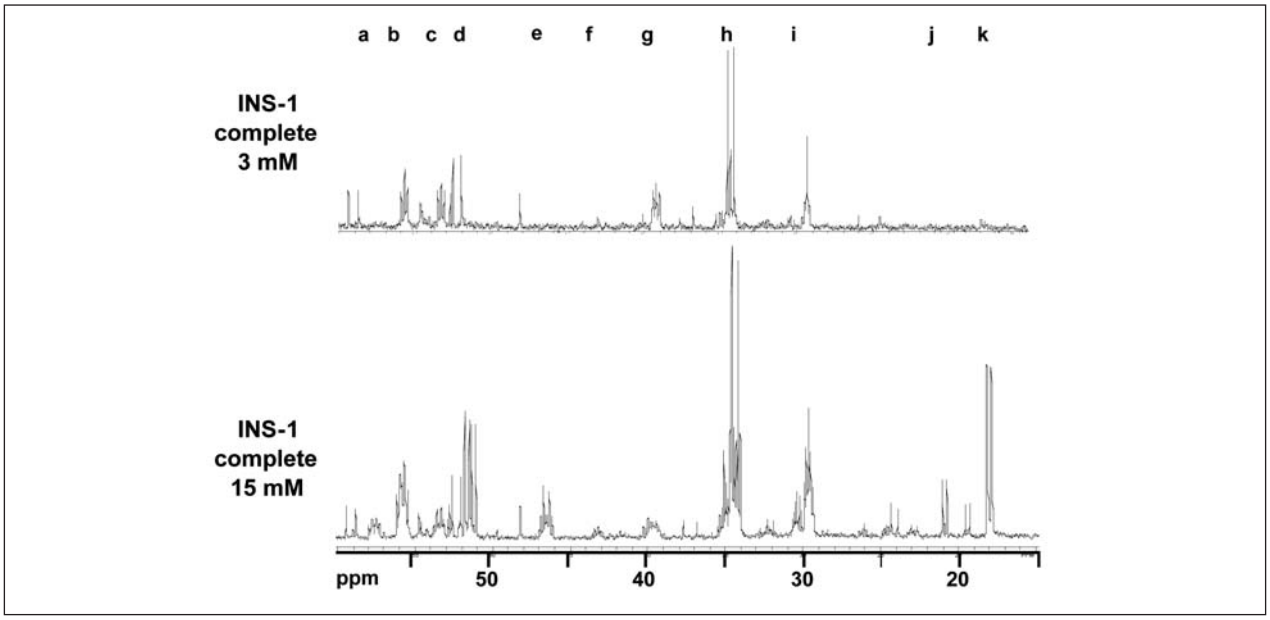

Figure 6. Representative proton-decoupled ^{13}C-NMR spectra obtained from extracts of INS-1 monolayer cultures exposed to complete media conditions containing 3 mM or 15 mM uniformly-labeled ^{13}C-glucose. Spectra are shown with equivalent S/N. On the x-axis at the bottom of the figure is the chemical shift region between 15 and 60 ppm. Species of interest are lettered, and include: (**a**) serine C2; (**b**) glutamate C2; (**c**) aspartate C2; (**d**) alanine C2; (**e**) citrate C2 & C4; (**f**) glycine C2; (**g**) aspartate C3; (**h**) glutamate C4; (**i**) glutamate C3; (**j**) lactate C3; and (**k**) alanine C3

their relative concentration, as depicted in Figure 6. In this figure, INS-1 cells were exposed to 3 mM or 15 mM glucose conditions in complete media, and large increases are observed in glutamate (b, h and i), serine (a), alanine (d and k), lactate (j), and citrate (e) resonances. Most of the remaining resonances show similar levels, with the notable exception of aspartate, whose labeled levels decreased under high glucose conditions (resonances c and g). Supporting the NMR isotopomer data are results of glucose consumption and insulin secretion under different media conditions. These also show an increase in response to glucose levels or media complexity. However, ATP/ADP levels were influenced more by glucose levels than by media complexity. It is important to note that this observation or similar correlations between cell bioenergetics and metabolism may be cell line dependent (35).

Conclusions to be gained from this study are that NMR spectroscopy can be used in concert with metabolic and secretory measurements to provide an understanding of the relationship between hormone secretion and cell energetics. Although in this case the secretory hormone was insulin, the same type of experiments can be performed with a variety of neuroendocrine cells. Most importantly, the composition of the incubation media impacts the metabolic and secretory ability of the cells as well as the ^{13}C isotopomer patterns. This is a critical take-home lesson for any study attempting to link cellular energetics with cellular function. Because media plays a significant role in the performance of the cells under study, and is easily manipulated, strict adherence to protocol is necessary to obtain meaningful information.

Study 2

A second important consideration when performing NMR isotopomer studies, regardless of the cell system under scrutiny, is how to best analyze the isotopomeric data through metabolic modeling. Following is an example of the impact that model selection has on data interpretation.

Defining pathways critical to insulin secretion in surrogate sources as well as native islets is a research

goal key towards discovering novel avenues of therapeutic intervention for diabetes. One reason is because determining paths critical to secretion would enable cellular engineers to tailor superior surrogate cells. Though the "Fuel Hypothesis" (22-25) links ISR to the oxidative metabolism of a variety of metabolic fuels, and is broadly accepted for islets, there are anomalies that the model cannot adequately address. Consequently, the importance of specific enzymatic pathways to insulin release is still under investigation (1-4, 36-38). Although NMR isotopomer analysis can obtain bioenergetic information through the study of the carbons of glutamate, choosing an appropriate metabolic model is of paramount importance when estimating metabolic data and correlating it with cellular function (in this case, ISR). Using ^{13}C isotopomer analysis to define a link between ISR and metabolic parameters, other workers have put forth a controversial two-pyruvate pool metabolic model (2), which although it allowed fitting of their isotopomer data, does not conform to the standard model of glucose metabolism (as depicted in Figure 1). Analysis of their isotopomer data with a dual-pyruvate pool model yielded a strong correlation between the insulin induction level and pyruvate cycling, a previously undocumented relationship. However, though there are possible mechanisms for compartmentation of metabolites (39-42), the dual-pool concept is controversial (43), and has not yet been robustly demonstrated to exist in native β-cells or insulinomas.

For this study, all the acquired data were fit by 'tcaCALC' using three different metabolic models: the two-pyruvate pool model (2) depicted in Figure 3B; a *'simple'* single-pyruvate pool model (Fig. 3A); and a *'modified'* single-pyruvate pool model, which has an additional carbon entrance via non-PC anaplerosis (Fig. 3A). A metabolic model's ability to derive useful information from isotopomer data was judged by how well the model-generated results reflected the measured isotopomeric fraction data (defined as the residual difference) and by how well the glutamate C3/C4 ratio was replicated (measured by the % C3/C4 error).

Table 1 details the model-specific residuals and % C3/C4 errors (when using the *'simple'* single-pyruvate pool, dual-pyruvate pool or *'modified'* pyruvate pool models) for the INS-1 cells and the media conditions under which they were tested. Isotopomeric analysis using 'tcaCALC' with the *'simple'* single-pyruvate pool model was the poorest of the three models under complete media conditions, as indicated by the large residual and % C3/C4 error shown in Table 1. This fitting anomaly, particularly evident in the observed % C3/C4 error when cells are exposed to complete media (reaching an error of over 115 %), suggests that the *'simple'* single-pyruvate pool model is insufficient to properly analyze data. The two-pyruvate pool model fit the data much better than the simple single-pyruvate pool model (i.e., reduced residuals and % C3/C4 errors), in all cases except for cells exposed to PBS containing 15 mM glucose. However, a major limitation of this model is that although the model allows for limited 'crossover' between the cycling secondary pyruvate pool and the primary pyruvate pool, pyruvate in the primary pool cannot enter the TCA cycle via

Table 1. Effect on the residual and % C3/C4 error when applying different models of metabolism (shown are results of applying *'simple'* single pyruvate pool, dual-pyruvate pool, and *'modified'* pyruvate pool models) to INS-1 cell extract data acquired under a variety of media conditions

		'simple' single pyruvate pool		dual-pyruvate pool		*'modified'* single pyruvate pool	
Cell Line	Media Conditions	residual	% C3/C4 error	residual	% C3/C4 error	residual	% C3/C4 error
INS-1	3 mM PBS	0.0561	4.25	0.0540	- 0.41	0.0557	1.38
	15 mM PBS	0.0101	7.93	0.0101	7.93	0.0086	0.17
	15 mM PBS	0.0260	17.63	0.0260	17.63	0.0048	4.40
	15 mM incomplete	0.1280	45.24	0.0012	- 1.99	0.0032	- 1.35
	15 mM incomplete	0.0850	33.33	0.0019	- 0.53	0.0009	- 0.83
	3 mM complete	0.1921	66.22	0.0266	- 0.32	0.0270	- 0.38
	3 mM complete	0.2885	115.66	0.0031	2.09	0.0048	2.14
	15 mM complete	0.1620	52.91	0.0053	- 3.30	0.0049	- 3.20
	15 mM complete	0.0617	25.23	0.0025	- 0.84	0.0037	- 0.13

Table 2. Statistical comparison of the residual and % C3/C4 error derived from the three applied models of metabolism. The t-test measures for differences between the values (smaller values are better), and the F-test is applied to determine differences in the scatter (less scatter is better). A single * denotes a statistical significance of $p<0.05$, and ** denotes $p<0.01$

		dual-pyruvate pool		'modified' single pyruvate pool	
		residual	% C3/C4 error	residual	% C3/C4 error
		0.0145 ± 0.0179	2.25 ± 6.60	0.0126 ± 0.0179	0.24 ± 2.19
'simple' single pool					
residual = 0.1122 ± 0.0898	t-test	*	*	*	**
% C3/C4 error = 40.93 ± 34.76	F-test	**	**	**	**
dual-pyruvate pool					
residual = 0.0145 ± 0.0179	t-test			N.S.	N.S.
% C3/C4 error = 2.25 ± 6.60		F-test		N.S.	**

PC. In essence, the cytosolic pyruvate has a 'memory' of its source and is metabolized by an appropriate enzyme. Analysis with the '*modified*' single-pyruvate pool model proved vastly superior to the simple single-pyruvate pool model and equal or superior to the two-pyruvate pool model under all conditions tested (measured by significantly reduced residuals and % C3/C4 errors, and tighter precision (i.e., scatter) of the residual and % C3/C4 error). Table 2 shows the results of direct comparative tests between the three models. Application of the dual-pyruvate pool model significantly reduced residuals and the % C3/C4 error (t-test; $p<0.05$), and the precision (scatter) of the residuals and the % C3/C4 error was significantly improved (F-test; $p<0.01$), compared to those derived from the *'simple'* single-pool model. Application of the *'modified'* single-pool model yielded similar improvements, and an even better reduction of the % C3/C4 error ($p<0.01$), when compared to the *'simple'* single pool model. The mean values obtained by the *'modified'* single-pool model are lower than those of the dual-pyruvate pool model, but statistically, there is no difference except in the great improvement of precision of the % C3/C4 error (F-test; $p<0.01$). As the *'modified'* model conforms to the standard model of metabolism and does not require any unproved characteristics, it was deemed the 'best' model for analysis of the isotopomer data. However, even though this model is arguably the best metabolic model for the cell line studied, subsequent analyses were performed with all three models to illustrate what type of information can be extracted from isotopomer analysis, even if the model applied is inappropriate.

Regardless of metabolic model applied, most correlations between GCR, ATP/ADP or ISR to model parameters (i.e., pyruvate cycling, anaplerosis through PC, non-PC anaplerosis, total anaplerosis and % anaplerotic carbon entry to the TCA cycle, etc.) from INS-1 cells exposed to a variety of conditions that alter metabolic and secretory activities were weak (data not shown). The critical correlations here are with the function of the cell, i.e., insulin secretion. The strongest correlations overall between insulin release and a modeled parameter (for each model tested) are represented in Table 3, which lists the Pearson product-moment correlation R values. The strongest relationship found when applying the 'simple' single-pyruvate pool model was between ISR and pyruvate cycling (R=0.488) or % anaplerosis (R=0.420), neither of which are particularly good correlations. The fact that this model is insufficient to properly fit the data (as described earlier) lends little support to these correlated

Table 3. Pearson product-moment correlations (R) between insulin release of INS-1 cells exposed to a variety of media conditions and parameters of metabolism derived from application of models of metabolism *('simple'* single-pyruvate pool; dual-pyruvate pool; *'modified'* single-pyruvate pool) to ^{13}C isotopomer data. N.A. indicates that the parameter is not applicable for that model

	Pyruvate cycling	Non-PC anaplerosis	% anaplerosis
'simple' single pyruvate pool	0.488	N.A.	0.420
dual-pyruvate pool	0.743	N.A.	0.793
'modified' single pyruvate pool	0.583	0.736	0.720

values. Correlations between ISR and parameters derived when applying the dual-pyruvate pool model were much improved for ISR vs. pyruvate cycling (R=0.743) or for ISR vs. % anaplerosis (R=0.793). Although as described above, the model fits the data well, it is not yet determined if dual-pyruvate pools can or do exist in this cell line. Nonetheless, these results suggest that anaplerosis plays an important role in insulin release, and corroborate observations made by Lu et al. in their studies with the INS-1 cell line. Application of the *'modified'* single-pyruvate pool model also shows a relationship between ISR and pyruvate cycling (R=0.583) or % anaplerosis (R=0.720), echoing that anaplerosis is a key player in the hormone release of this cell line. Importantly, an additional observation is obtained by the application of the *'modified'* single-pyruvate pool model, namely that non-PC anaplerosis correlates well with insulin release (R=0.736). This suggests an entirely new avenue of research.

The data suggests a complex relationship between ISR and modeled parameter of metabolism (e.g., non-PC anaplerosis in the *'modified'* single-pyruvate pool model). To address this complexity, we tested the change in model-derived parameters vs. the change in ISR under conditions that induce the ISR changes. Composition changes included: 3mM glucose PBS vs. 15 mM PBS; 3 mM glucose complete media vs. 15 mM glucose complete media; 3 mM glucose PBS vs. 3 mM glucose complete media; and 15 mM glucose PBS vs. 15 mM glucose complete media. When using the most appropriate 'modified' single-pyruvate pool model, the Pearson product-moment correlation was strongest between the change in ISR vs. the change in non-PC anaplerosis (R=0.910) and again suggests that a change in non-PC anaplerosis plays a key role in secretion. It also corroborates recent studies linking anaplerotic substrates to insulin secretion (44), and begs the question "What is the potential source of the non-PC anaplerosis?".

There are two major candidates for this source: glutamate (which could enter the TCA cycle after conversion to αKG), and aspartate (which could enter the TCA cycle after conversion to OAA). These amino acids are readily labeled upon incubation with labeled glucose, as observed by inspection of Fig. 4. The role of glutamate in insulin release has been debated (45), but is now thought not to play a direct role (46, 47). We have recently hypothesized that the key non-PC anaplerotic substrate is aspartate (48), and a manuscript regarding this is in preparation. Further evidence of an association between aspartate and insulin release involves aspartate aminotransferase. When an inhibitor of aspartate aminotransferase (aminooxyacetate) is introduced, insulin secretion stimulated by succinate esters is not affected. However, this compound is known to completely inhibit glucose-stimulated insulin secretion (49). In other words, when aspartate levels are not allowed to drop, insulin release is inhibited.

To summarize, this study demonstrates that identifying the appropriate model of metabolism is key in the interpretation of the isotopomer patterns and the subsequent extraction of enzymatic fluxes. This exercise points to the fact that it is possible that more than one model may have the statistical power to fit the data. Here, a robust *'modified'* single-pyruvate pool metabolic model and a non-conventional two-pyruvate pool model provided essentially the same excellent fits to isotopomer data derived from INS-1 cells exposed to a wide variety of media conditions. However, different critical pathways are suggested by the models, warranting further studies to validate the most appropriate model.

Conclusion

By considering the above studies, it should be apparent how NMR spectroscopic studies similar to those outlined here may be of great importance to the study of pituitary adenomas. For example, one could determine the efficacy of a host of metabolic modulators. Or conversely, one may observe the metabolic effects of a known modulator of cell function, to glean insight to links between metabolism and cell function. If a pituitary adenoma has biochemical machinery that differs sufficiently from normal tissue, one may have exploitable differences in metabolism that will present an opportunity or a target for successful therapeutic intervention. Therefore, although no definitive studies on the metabolic fate of labeled carbons in adenomas have been yet performed, there are many

new avenues for exploration towards defining critical metabolic pathways related to hormone release. However, caution is offered to perform the experiments with the most physiologically relevant media and choose appropriate metabolic models to assure that the results obtained are valid and relevant to the actual physiology of the pituitary adenoma under study. With proper application of powerful NMR spectroscopic techniques, important information regarding cellular energetics of pituitary adenomas will be determined.

Acknowledgements

The authors are grateful for the technical assistance of Jose Oca-Cossio, Chiab Simpson, Nata Khokhlova and Carol Sweeney. This work was supported by grants from the NIH (DK56890, DK47858). The program 'tcaCALC' was obtained from the University of Texas Southwestern, and developed through H-47669-16 and RR-02584. NMR data were obtained at the Advanced Magnetic Resonance Imaging and Spectroscopy (AMRIS) facility in the McKnight Brain Institute of the University of Florida.

References

1. Brennan L, Shine A, Hewage C, et al. A nuclear magnetic resonance-based demonstration of substantial oxidative L-alanine metabolism and L-alanine-enhanced glucose metabolism in a clonal pancreatic β-cell line. *Diabetes* 2002; 51: 1714-21.
2. Lu DH, Mulder H, Zhao P, et al. ^{13}C NMR isotopomer analysis reveals a connection between pyruvate cycling and glucose-stimulated insulin secretion (GSIS). *Proc Nat Acad Sci* 2002; 99: 2708-13.
3. Brennan L, Corless M, Hewage C, et al. ^{13}C NMR analysis reveals a link between L-glutamine metabolism, D-glucose metabolism and γ-glutamyl cycle activity in a clonal pancreatic beta-cell line. *Diabetologia* 2003; 46: 1512-1521.
4. Cline GW, LePine RL, Papas KK, Kibbey RG, Shulman GI. ^{13}C-NMR isotopomer analysis of anaplerotic pathways in INS-1 cells. *J Biol Chem* 2004; 279: 44370-5.
5. Portais JC, Schuster R, Merle M, Canioni P. Metabolic flux determination in C6 glioma cells using carbon-13 distribution upon [1-^{13}C] glucose incubation. *Eur J Biochem* 1993; 217: 457-68.
6. Constantinidis I, Sambanis A. Towards the development of artificial endocrine tissues: ^{31}P NMR spectroscopic studies of immunoisolated insulin-secreting AtT-20 cells. *Biotechnol Bioeng* 1995; 47: 431-43.
7. Papas KK, Long RCJ, Constantinidis I, Sambanis A. Role of ATP and P_i in the mechanism of insulin secretion in the mouse insulinoma βTC3 cell line. *Biochem J* 1997; 326: 807-14.
8. Constantinidis I, Sambanis A. Noninvasive monitoring of tissue-engineered constructs by nuclear magnetic resonance methodologies. *Tissue Engin* 1998; 4: 9-17.
9. Papas KK, Colton CK, Gounarides JS, et al. NMR spectroscopy in beta cell engineering and islet transplantation. *Ann NY Acad Sci* 2001; 944: 96-119.
10. Mancuso A, Beardsley NJ, Wehrli S, Pickup S, Matschinsky FM, Glickson JD. Real-time detection of ^{13}C NMR labeling kinetics in perfused EMT6 mouse mammary tumor cells and βHC9 mouse insulinomas. *Biotechnol Bioeng* 2004; 87: 835-848.
11. Stacpoole PW, Simpson NE, Han Z, Kerr DS, Constantinidis I. NMR spectroscopy identifies biochemical consequences of pyruvate dehydrogenase complex deficiency and its treatment in cultured human fibroblasts. Society for the Study of Inborn Errors of Metabolism, 41st Annual Symposium, Amsterdam, The Netherlands, 2004; Abstract 240-O.
12. Farrar TC, Becker ED. Pulse and Fourier Transform NMR. New York; Academic Press,1971.
13. Gadian DG. Nuclear magnetic resonance and its application to living systems. New York; Oxford University Press, 1982.
14. Stryer L. Biochemistry. New York; W. H. Freeman and Company, 1988.
15. Lehninger AL, Nelson DL, Cox MM. Principles of biochemistry. New York; Worth Publishers, 1993.
16. Malloy CR, Sherry AD, Jeffrey FMH. Evaluation of carbon flux and substrate selection through alternative pathways involving the citric acid cycle of the heart by ^{13}C-NMR spectroscopy. *J Biol Chem* 1988; 263: 6964-71.
17. Malloy CR, Sherry AD, Jeffrey FMH. Analysis of tricarboxylic acid cycle of the heart using ^{13}C isotope isomers. *Am J Physiol* 1990; 259: H987-H995.
18. Sherry AD, Jeffrey FMH, Malloy CR. Analytical solutions for ^{13}C isotopomer analysis of complex metabolic conditions: substrate oxidation, multiple pyruvate cycles, and gluconeogenesis. *Metabol Engin* 2004; 6: 12-24.
19. Gunawardana SC, Sharp GWG. Intracellular pH plays a critical role in glucose-induced time-dependent potentiation of insulin release in rat islets. *Diabetes* 2002; 51: 105-13.
20. Simpson NE, Bennett LK, Papas KK, Sambanis A, Constantinidis I. Effects of pH on murine insulinoma βTC3 cells. Biochem Biophys Res Comm 2000; 273: 937-41.
21. Tyagi RK, Azrad A, Degani H, Salomon Y. Simultaneous extraction of cellular lipids and water-soluble metabolites: Evaluation by NMR spectroscopy. *Magn Reson Med* 1996; 35: 194-200.
22. Malaisse WJ, Sener A, Herchuelz A, Hutton JC. Insulin release: the fuel hypothesis. *Metabolism* 1979; 28: 373-85.
23. Newgard CB, McGarry JD. Metabolic coupling factors in pancreatic β-cell signal transduction. *Ann Rev Biochem* 1995; 64: 689-719.

24. Matschinsky FM. A lesson in metabolic regulation inspired by the glucokinase glucose sensor paradigm. *Diabetes* 1996; 45: 223-41.
25. Prentki M. New insights into pancreatic β-cell metabolic signaling in insulin secretion. *Eur J Endocrin* 1996; 134: 272-86.
26. Jans AWH, Willem R. A ^{13}C NMR study of the application of [U-^{13}C]succinate for metabolic investigations in rabbit renal proximal convoluted tubular cells. *Magn Reson Med* 1990; 14: 148-53.
27. Malaisse WJ, Zhang T-M, Vaerbruggen I, Willem R. D-glucose generation from [2-^{13}C]pyruvate in rat hepatocytes: implications in terms of enzyme-to-enzyme channeling. *Arch Biochem Biophys* 1996; 332: 341-51.
28. Muller TB, Sonnewald U, Westergaard N, Schousboe A, Petersen SB, Unsgard G. ^{13}C NMR spectroscopy study of cortical nerve cell cultures exposed to hypoxia. *J Neurosci Res* 1994; 38: 319-26.
29. Brand A, Engelmann J, Leibfritz D. A ^{13}C NMR study on fluxes into the TCA cycle of neuronal and glial tumor cell lines and primary cells. *Biochimie* 1992; 74: 941-8.
30. Lutz NW, Yahi N, Fantini J, Cozzone PJ. A new method for the determination of specific ^{13}C enrichment in phosphorylated [1-^{13}C]glucose metabolites. *Eur J Biochem* 1996; 238: 470-5.
31. Martin M, Portais J-C, Voisin P, Rousse N, Canioni P, Merle M. Comparative analysis of ^{13}C-enriched metabolites released in the medium of cerebellar and cortical astrocytes incubated with [1-^{13}C]glucose. *Eur J Biochem* 1995; 231: 697-703.
32. Sonnewald U, White LR, Odegard E, et al. MRS study of glutamate metabolism in cultured neurons/glia. *Neurochem Res* 1996; 21: 987-93.
33. Hamid M, McCluskey JT, McClenaghan NH, Flatt PR. Comparative functional study of clonal insulin-secreting cells cultured in five commercially available tissue culture media. *Cell Transplant* 2001; 10: 153-9.
34. Sekine N, Fasolato C, Pralong WF, Theler JM, Wollheim CB. Glucose-induced insulin secretion in INS-1 cells depends on factors present in fetal calf serum and rat islet-conditioned media. *Diabetes* 1997; 46: 1424-33.
35. Simpson NE, Khokhlova N, Oca-Cossio JA, Constantinidis I. Media-influenced secretory and ^{13}C isotopomer behavior of insulinoma cells. The International Society of Magnetic Resonance in Medicine, 12th Annual Meeting, Kyoto, Japan, 2004; Abstract 2026.
36. Farfari S, Schulz V, Corkey B, Prentki M. Glucose-regulated anaplerosis and cataplerosis in pancreatic β-cells: possible implication of a pyruvate/citrate shuttle in insulin secretion. *Diabetes* 2000; 49: 718-726.
37. Fahien LA, MacDonald MJ. The succinate mechanism of insulin release. *Diabetes* 2002; 51: 2669-76.
38. Rocheleau JV, Head WS, Nicholson WE, Powers AC, Piston DW. Pancreatic islet β-cells transiently metabolize pyruvate. *J Biol Chem* 2002; 277: 30914-20.
39. Mowbray J, Ottaway JH. The effect of insulin and growth hormone on the flux of tracer from labelled lactate in perfused rat hearts. *Eur J Biochem* 1973; 36: 369-379.
40. Peuhkurinen KJ, Hiltunen JK, Hassinen IE. Metabolic compartmentation of pyruvate in the isolated perfused rat heart. *Biochem J* 1983; 210: 193-8.
41. Brooks GA, Dubouchaud H, Brown M, Sicurello JP, Butz CE. Role of mitochondrial lactate dehydrogenase and lactate oxidation in the intracellular lactate shuttle. *Proc Natl Acad Sci* 1999; 96: 1129-34.
42 Gladden LB. Lactate metabolism: a new paradigm for the third millennium. *J Physiol* 2004; 558: 5-30.
43. Sahlin K, Fernstrom M, Svensson M, Tonkonogi M. No evidence of an intracellular lactate shuttle in rat skeletal muscle. *J Physiol* 2002; 541: 569-74.
44. MacDonald MJ, Fahien LA, Brown LJ, Hasan NM, Buss JD, Kendrick MA. Perspective: emerging evidence for signaling roles of mitochondrial anaplerotic products in insulin secretion. *Am J Physiol Endocrinol Metab* 2005; 288: E1-E15.
45. Maechler P, Wollheim CB. Mitochondrial glutamate acts as a messenger in glucose-induced insulin exocytosis. *Nature* 1999; 402: 685-9.
46. Bertrand G, Ishiyama N, Nenquin M, Ravier MA, Henquin JC. The elevation of glutamate content and the amplification of insulin secretion in glucose-stimulated pancreatic islets are not causally related. *J Biol Chem* 2002; 277: 32883-91.
47. MacDonald MJ, Fahien LA. Glutamate is not a messenger in insulin secretion. *J Biol Chem* 2000; 275: 34025-7.
48. Simpson NE, Oca-Cossio JA, Khokhlova N, Constantinidis I. ^{13}C isotopomer studies of insulin-secreting cells: anaplerosis plays a role. The International Society of Magnetic Resonance in Medicine, 13th Annual Meeting, Miami Beach, FL, 2005; Abstract 830.
49. MacDonald MJ, Fahien LA, Mertz RJ, Rana R. Effect of esters of succinic acid and other citric acid cycle intermediates on insulin release and inositol phosphate formation by pancreatic islets. *Arch Biochem Biophys* 1989; 269: 400-6.

Correspondence: Nicholas E. Simpson, PhD,
Division of Endocrinology
1600 SW Archer Rd., PO Box 100226,
Gainesville, FL 32610-0226
Tel. (352) 846-2723
Fax: (352) 846-2635
E-mail: simpsn@medicine.ufl.edu